

Gate-tunable nearly total terahertz absorption in graphene with resonant metal back reflector

Jiang-Tao Liu,^{1, 2,*} Nian-Hua Liu,^{1, 2} Li Wang,^{1, 2} Xin-Hua Deng,² and Fu-Hai Su^{3, †}

¹*Nanoscale Science and Technology Laboratory, Institute for Advanced Study, Nanchang University, Nanchang 330031, China*

²*Department of Physics, Nanchang University, Nanchang 330031, China*

³*Key Laboratory of Materials Physics, Institute of Solid State Physics, Chinese Academy of Sciences, Hefei 230031, China*

(Dated: September 8, 2018)

The gate-tunable terahertz (THz) absorption of graphene layers with a resonant metal back reflector (RMBF) is theoretically investigated. We demonstrate that the THz absorption of graphene with RMBF can vary from nearly negligible to nearly total by tuning the external gate voltage. This peculiar nearly total THz absorption can be attributed to the Fabry-Perot cavity effect, which enhances the absorption and reduces the reflection of graphene. The absorption spectra of the graphene-RMBF structure can also be tailored in bandwidth and center frequency by changing the thickness and dielectric constant of the spacer layer.

PACS numbers: 78.67.Wj Optical properties of graphene, 95.85.Fm Submillimeter (300 μm -1 mm), 42.25.Bs Wave propagation, transmission and absorption

The optical properties of graphene is attracting increased attention because of the abundant potential applications within a wide spectral range from terahertz (THz) to visible frequencies [1–24]. As an ultra-thin two-dimensional (2D) carbon material, graphene is widely used in the transparent electrodes and optical display materials [1–4]. In recent years, THz techniques have been used to study the electric states in graphene [25–30]. Given the ultra-high carrier mobility of graphene, it also has applications in THz optoelectronics such as transformation optics [23], tunable THz modulators [31–35], room-temperature THz detectors [36], THz optical antennas [37], etc. These graphene-based THz devices have important applications, such as in medical diagnostics, molecular biology, and homeland security.

To promote the applications of graphene within the THz frequency range, the interaction between graphene and THz waves should be enhanced. In the recent two years, various graphene plasmonics with different microstructures have been proposed to enhance the absorption of graphene [12–21]. In particular, nearly complete absorption can be achieved in periodically patterned graphene or microcavity [12, 13]. The concept of perfect absorbers has initiated a new research area and has important applications in optoelectronics [12, 38–40]. However, fabricating periodically patterned graphene or placing it in an optical microcavity under current technological conditions remains difficult.

Recently, Liu et al. proposed that the optical absorption of graphene layers on the top of a one-dimensional photonic crystal (1DPC) can be significantly enhanced within the visible spectral range because of photon localization [41]. In a similar manner, the absorption of

graphene can also be increased within the THz spectra range [42]. The proposed 1DPC structures can be implemented using existing technologies. However, the photonic band gap (PBG) of 1DPC limits the spectrum bandwidth for the absorption enhancement of graphene. In fact, highly conducting metal films such as aluminum, silver, and gold can effectively reflect the electromagnetic wave within a wide spectral range from the middle-infrared region to the microwave region the same as a 1DPC [43]. Thus, the metal film can replace the 1DPC to enhance the THz absorption of graphene within a wide spectrum region. Apart from performing as the back reflector, the metal film can also act as the metal gate electrode that can be used to modulate graphene absorption.

In this Letter, the THz absorption of graphene layer prepared on top of $\text{SiO}_2/\text{p-Si}$ substrate with a resonant metal back reflector (RMBF) is theoretically investigated. We find that the absorption of graphene with an RMBF can be enhanced by about 3.3 times because of Fabry-Perot interference. The full width at half maximum of the absorption spectrum (FWHM) of graphene with an RMBF is much larger than that of graphene on top of a 1DPC. By tuning the applied gate voltage, the THz absorption of graphene layer with an RMBF can vary from nearly total transparency to total absorption regardless of the incident angle if this angle is not too large. Our proposal is very easy to implement using the existing technology and has potential important applications in both THz and graphene studies.

The details of the structure are shown in the inset of Fig. 1. The spacer layers consist of 300 nm SiO_2 layers and a 21.9 μm lightly doped p-type silicon (p-Si) layer with resistivity greater than 100 $\Omega \text{ cm}$, unless otherwise specified. The graphene layer is prepared on top of the SiO_2 layer, and an 86 nm silver film is placed at the bottom of the p-Si layer as the back reflector and metal gate electrode [44]. The refractive index of the p-Si (SiO_2) layer is 3.418 (2.1) and negligible in THz absorption [45].

*Electronic address: jtliu@semi.ac.cn

†Electronic address: fhsu@issp.ac.cn

The conductivity of Ag film is $\sigma_{Ag} = 46(\mu\Omega)^{-1}$, and the complex refractive index is $n_{Ag} = (1+i)\sqrt{\sigma_{Ag}/(4\pi\varepsilon_0 f)}$, where ε_0 is the vacuum dielectric constant, and f the THz wave frequency [43]. Within the THz frequency range, the conductivity of graphene can be expressed as [42]

$$\sigma_g = \frac{e^2}{\pi\hbar} \frac{|\epsilon_F|}{\hbar\Gamma - i\hbar\omega}, \quad (1)$$

where \hbar is the reduced Planck constant, Γ is the relaxation rate, ϵ_F is the Fermi level position with respect to the Dirac point, and ω is the angular frequency of the incident THz radiation.

To model the THz absorption of graphene in this structure, the transfer matrix method is used [41, 46, 47]. The electric field of the TE mode and the magnetic field of the TM mode of THz waves in the l th layer is given by $E_l(y, z) = (A_l e^{ik_z z} + B_l e^{-ik_z z}) e^{-ik_y y} e_x$ and $H_l(y, z) = (A_l e^{ik_z z} + B_l e^{-ik_z z}) e^{-ik_y y} e_x$, respectively. Where the TM (TE) mode is defined as the component of the magnetic (electric) field parallel to the graphene layers. The relation of the electromagnetic field in the l th layer to the incident electromagnetic wave is

$$\begin{pmatrix} A_l \\ B_l \end{pmatrix} = \begin{pmatrix} T_{11} & T_{12} \\ T_{21} & T_{22} \end{pmatrix} \begin{pmatrix} A_0 \\ B_0 \end{pmatrix}. \quad (2)$$

Thus, we can obtain the absorbance of graphene \mathcal{A}_o using the Poynting vector [41]

$$\mathcal{A}_o = (\mathcal{S}_{0i} + \mathcal{S}_{2i} - \mathcal{S}_{0o} - \mathcal{S}_{2o})/\mathcal{S}_{0i}, \quad (3)$$

where \mathcal{S}_{0i} and \mathcal{S}_{0o} (\mathcal{S}_{2i} and \mathcal{S}_{2o}) are the incident and outgoing Poynting vectors in air (in the nearest spacer layer), respectively. Here, $\mathcal{S}_{0i} = \beta_0 A_0^2 \cos \theta$, $\mathcal{S}_{0o} = \beta_0 B_0^2 \cos \theta$, $\mathcal{S}_{2i} = \beta_1 B_2^2 \cos \theta'$, and $\mathcal{S}_{2o} = \beta_1 A_2^2 \cos \theta'$. For the TE mode, $\beta_0 = \sqrt{\varepsilon_0/\mu_0}$, $\beta_1 = \sqrt{\varepsilon_s/\mu_0}$; for the TM mode, $\beta_0 = \sqrt{\mu_0/\varepsilon_0}$, $\beta_1 = \sqrt{\mu_0/\varepsilon_s}$, where ε_s is the dielectric constant of the spacer layer, and θ' is the propagation angle of light in the spacer layer.

Figure 1 shows the THz absorption of graphene layers under normal incidence in different structures as a function of frequency. In the calculations, $\hbar\Gamma = 2.5$ meV and $\varepsilon_F = 0.06$ eV are used. The maximum THz absorbance of the graphene monolayer with an RMBF is about 0.5 (red dashed line in Fig. 1). By contrast, for the same frequency ($f \approx 1$ THz), the absorbance of the suspended graphene monolayer is about 0.15 (black solid line in Fig. 1). Thus, the absorption of graphene monolayer with an RMBF can be enhanced by about 3.3 times. For three graphene monolayers, a maximum THz absorbance of 0.85 can be achieved (dash-dot-dotted line in Fig. 1). Similar to graphene with a 1DPC, the graphene layer and the metal film act as the mirrors of the Fabry-Perot Cavity. The THz wave propagates back and forth between these two mirrors, which leads to photon localization and enhances the absorption of graphene [41, 47].

In Fig. 1, we also show the THz absorption of graphene layers prepared on top of 7.5 period alternating Si and

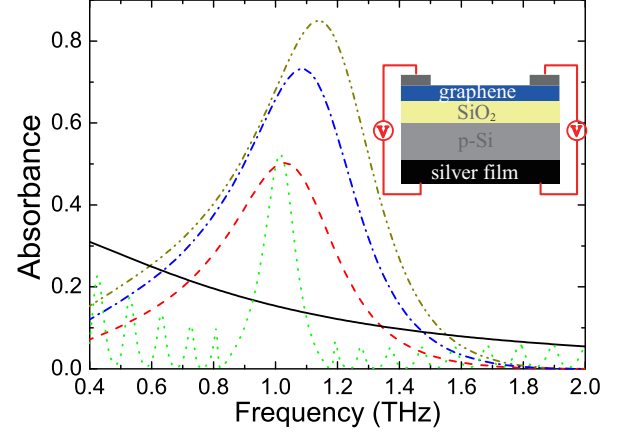


FIG. 1: (color online) The absorbance of graphene as a function of the frequency for different structures: suspended graphene monolayer (black solid line), graphene monolayer with a 1DPC (green dotted line), graphene monolayer with an RMBF (red dashed line), two graphene monolayers with an RMBF (blue dash-dotted line), and three graphene monolayers (dark yellow dash-dot-dotted line). The inset shows the schematic of the graphene layer prepared on top of SiO₂/p-Si spacer layers with an RMBF.

SiO₂ layers, i.e., 1DPC. The maximum THz absorbance of the graphene monolayer with a 1DPC is about 0.52 (green dotted line in Fig. 1), which is slightly larger than that of the graphene monolayer with an RMBF. However, the FWHM of the absorption spectrum of graphene monolayer with a 1DPC is only about 0.11 THz limited to the PBG width in 1DPC. By contrast, the bandwidth of absorption in the graphene-RMBF structure can reach 0.45 THz because the metal film can perfectly reflect the electromagnetic wave within the wide spectral range. More importantly, graphene-RMBF structure is much easier to realize than other proposed structures such as 1DPC, periodically patterned graphene, and microcavity. THz spectroscopy is also used to detect electron states and ultrafast dynamics of Dirac fermions in graphene [25–30]. The enhanced THz absorption with an RMBF can promote these studies and may help observe the THz-induced nonlinear dynamics of Dirac fermions in graphene [30, 48].

The THz absorption of graphene layers can be tuned by varying the gate voltage. The Fermi energy $|\varepsilon_F|$ of graphene can be continuously tuned by varying the gate-voltage similar to a field-effect transistor. As shown in Eq. (1), the conductivity of graphene is expected to increase as the Fermi energy $|\varepsilon_F|$ is increased, which enhances the intraband THz absorption of graphene. By using a simple capacitor model, the Fermi energy $|\varepsilon_F|$ of graphene in our proposed structure can be written as [5, 32]

$$|\varepsilon_F| = \hbar v_F \sqrt{\pi |\alpha_c(V_g - V_{E0})|}, \quad (4)$$

where $v_F = 1 \times 10^6$ m/s is the Fermi velocity, $\alpha_c \approx$

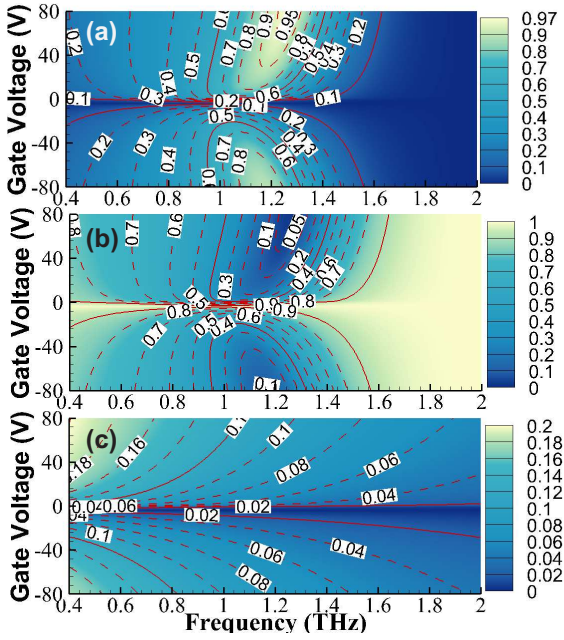


FIG. 2: (color online). Contour plots of the (a) absorbance and (b) reflectance of graphene monolayer with an RMBF as a function of the light frequency and back gate voltage. (c) Contour plots of the absorbance of graphene monolayer without an RMBF as a function of the light frequency and back gate voltage.

$7 \times 10^{10} \text{ cm}^{-2} \text{V}^{-1}$, $V_{E0} = \varepsilon_{F0}^2 / (\hbar^2 v_F^2 \pi \alpha_c)$, and ε_{F0} is the Fermi energy of graphene with zero gate-voltage.

The absorbance and reflectance of graphene monolayer with an RMBF as a function of the light frequency and back gate voltage for $\varepsilon_{F0} = 0.06 \text{ eV}$ are shown in Fig. 2(a) and 2(b), respectively. The absorbance of graphene with an RMBF can vary from nearly zero to nearly 100% by tuning the gate voltage. For instance, when $f = 1.26 \text{ THz}$, the absorbance (reflectance) of graphene with an RMBF for $V_g = 3.8 \text{ V}$, $V_g = 45 \text{ V}$, and $V_g = 80 \text{ V}$ is about 0.03 (0.96), 0.9 (0.08), and 0.97 (0.02), respectively. Thus, the absorbance and reflectance are very sensitive to the gate-voltage. By contrast, the absorbance of the graphene monolayer without an RMBF as a function of optical frequency and the back gate voltage is shown in Fig. 2(c). To remove the Fabry-Perot cavity effect, the thickness of the p-Si layer is set to semi-infinite. The maximum absorbance of graphene without an RMBF is only about 0.2, which is even smaller than that of suspended graphene monolayer (black solid line in Fig. 1). Thus, the traditional substrate material reduces the absorption of graphene. In fact, the absorption coefficient of graphene within the THz frequency range is large. The weak absorbance of graphene is due to the fact that most of the incident THz wave is reflected because of the large real and imaginary parts of the conductivity of graphene for a large Fermi energy $|\varepsilon_F|$ [49]. A resonant back reflector such as 1DPC or metal can reduce the reflection of graphene [47, 50] and lead to relatively weak photon

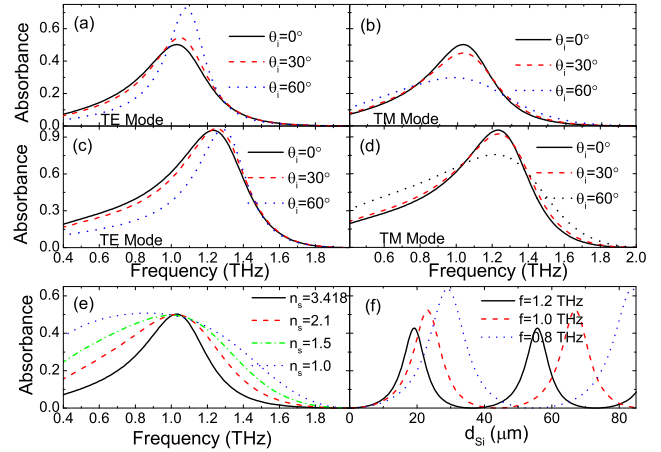


FIG. 3: (color online). Absorbance of graphene monolayer with an RMBF as a function of the light frequency for different incident angles: (a, b) $\varepsilon_F = 60 \text{ meV}$, and (c, d) $\varepsilon_F = 300 \text{ meV}$. Absorbance of graphene monolayer with an RMBF as a function of (e) the light frequency with different spacer layers and (f) the thickness of p-Si spacer layer.

localization [41], which are the key points for achieving nearly total THz absorption in graphene.

The absorption spectra of the graphene-RMBF structure in the case of oblique incidence of a THz beam are shown in Fig. 3. The resonance condition of a Fabry-Perot cavity can be described as $2L_o k \cos \theta' = 2m\pi$, where m is an integer, L_o is the optical path of the p-Si and SiO₂ spacer layers, k is the wave vector of the THz wave, and θ' is the propagation angle of the THz wave in the spacer layer. According to Snell's law, θ' is small even with a large incident angle θ_i because of the large refractive index of the p-Si layer in the proposed structure. Different from the 1DPC, the reflection of the metal films within the THz range is nearly invariable with increased incident angle. Thus, the THz absorption of graphene with an RMBF is less affected by the incident angle of the THz beams if the incident angle is not too large. For instance, for $\varepsilon_F = 300 \text{ meV}$, the absorbance of graphene monolayer for $\theta_i = 0^\circ$ and $\theta_i = 30^\circ$ for TE (TM) mode is about 0.956 (0.956) and 0.972 (0.926). Even for incident angle $\theta_i = 60^\circ$, the absorbance of graphene monolayer for the TE (TM) mode is about 0.963 (0.757). Thus, our proposed graphene-RMBF structure can be used in pанoscopic and imageable THz detectors and modulators.

We now consider the adjustability of the THz absorption of graphene by varying the dielectric constant or optical path of the spacer layers. The reflection of the graphene layer is smaller with a lower dielectric constant substrate, and the THz absorption of graphene is enhanced beyond the resonance cavity frequency. The FWHM of the THz absorption spectra increases with decreased dielectric constant of the spacer layers [see Fig. 3(e)]. For the normal incidence case, the resonance condition of a Fabry-Perot cavity is $2L_o k = 2m\pi$, which indicates that the center frequency of the absorption

spectra can be easily tuned by varying the spacer layers thickness. As shown in Fig. 3(f), the center frequency of the THz absorption peak increases with decreased spacer layers thickness. Given that the absorption coefficient of graphene is larger for lower frequency THz waves according to Eq. (1), the maximum absorption of graphene increases with increased spacer layers thickness. Thus, the fabrication of graphene-RMBF structure with a thickness-tunable air spacer layer (e.g., gate controlled suspended graphene [51, 52]) is also highly desired.

In summary, the gate-tunable THz absorption of graphene layers with an RMBF is investigated. The THz absorption of graphene with an RMBF is enhanced and can be tuned from nearly zero to nearly total by varying the gate voltage. This peculiar nearly total THz absorption can be attributed to the Fabry-Perot cavity effect, which enhances the absorption of graphene and reduces the reflection of the THz beams. The maximum absorp-

tion of graphene is almost unchanged even when the incident angle varies from 0° to 30° . The center frequency and FWHM of the absorption spectra can also be tuned by varying the thickness and dielectric constant of the spacer layers. Using existing technology, the proposed structure is very easy to fabricate not only in laboratory scale but also in industrial scale. Our findings have important implications in the development of THz photonic devices such as THz detectors and modulators, as well as in studies on the ultrafast dynamics of Dirac fermions in graphene.

This work was supported by the National Key Basic Research Program of China (2013CB934200), the NSFC Grant Nos. 11104232, 11264030, and 11364033, the NSF from the Jiangxi Province Nos. 20122BAB212003, and Science and Technology Project of Education Department of Jiangxi Province No. GJJ13005.

[1] F. Bonaccorso, Z. Sun, T. Hasan, and A. C. Ferrari, *Nature Photonics* **4**, 611-622 (2010).

[2] K. S. Kim, Y. Zhao, H. Jang, S. Y. Lee, J. M. Kim, K. S. Kim, J. H. Ahn, P. Kim, J. Y. Choi, and B. H. Hong, *Nature* **457**, 706-710 (2009).

[3] X. Wang, L. J. Zhi, and K. Mülen, *Nano Lett.* **8**, 323 (2008).

[4] S. Bae, H. Kim, Y. B. Lee, X. F. Xu, J. S. Park, Y. Zheng, J. Balakrishnan, T. Lei, H. R. Kim, Song, Y. I. Y. J. Kim, and K. S. Kim, B. Özyilmaz, J. H. Ahn, B. H. Hong, and S. Iijima, *Nat. Nanotechnol.* **5**, 574 (2010).

[5] F. Wang, Y. Zhang, C. Tian, C. Girit, A. Zettl, M. Crommie, and Y. R. Shen, *Science* **320**, 206-209 (2008).

[6] N. M. R. Peres, R. M. Ribeiro, and A. H. C. Neto, *Phys. Rev. Lett.* **105**, 055501 (2010).

[7] M. Liu, X. Yin, E. U. Avila, B. Geng, T. Zentgraf, L. Ju, F. Wang, and X. Zhang, *Nature* **474**, 64-67 (2011).

[8] Z. Z. Zhang, K. Chang, and F. M. Peeters, *Phys. Rev. B* **77**, 235411 (2008).

[9] P. H. Tan, W. P. Han, W. J. Zhao, Z. H. Wu, K. Chang, H. Wang, Y. F. Wang, N. Bonini, N. Marzari, N. Pugno, G. Savini, A. Lombardo, and A. C. Ferrari, *Nature Materials*, **11**, 294-300 (2012).

[10] Z. Fang, Z. Liu, Y. Wang, P. M. Ajayan, P. Nordlander, and N. J. Halas, *Nano Lett.* **12**, 3808-3813 (2012).

[11] N. Jung, A. C. Crowther, N. Kim, P. Kim, and L. E. Brus, *ACS Nano* **4**, 7005-7013 (2010).

[12] S. Thongrattanasiri, F. H. L. Koppens, and F. J. G. Abajo, *Phys. Rev. Lett.* **108**, 047401 (2012).

[13] A. Ferreira, N. M. R. Peres, R. M. Ribeiro, and T. Stauber, *Phys. Rev. B* **85**, 115438 (2012).

[14] M. Engel, M. Steiner, A. Lombardo, A. C. Ferrari, H. V. Loeheynes, P. Avouris, and R. Krupke, *Nature Communications* **3**, 906 (2012).

[15] A. N. Grigorenko, M. Polini, and K. S. Novoselov, *Nature Photonics* **6**, 749-758 (2012).

[16] Z. Fang, S. Thongrattanasiri, A. Schlather, Z. Liu, L. Ma, Y. Wang, P. Ajayan, P. Nordlander, and N. J. Halas, *ACS Nano* **7**, 2388-2395 (2013).

[17] S. Thongrattanasiri and F. J. G. Abajo, *Phys. Rev. Lett.* **110**, 187401 (2013).

[18] X. Zhu, W. Yan, P. U. Jepsen, O. Hansen, N. A. Mortensen, and S. Xiao, *Appl. Phys. Lett.* **102**, 131101 (2013).

[19] H. Yan, X. Li, B. Chandra, G. Tulevski, Y. Wu, M. Freitag, W. Zhu, P. Avouris and F. Xia, *Nature Nanotechnology* **7**, 330-334 (2012).

[20] J. L. G. Pomar, A. Y. Nikitin, and L. M. Moreno, *ACS Nano*, **7**, 4988-4994 (2013).

[21] X. Zhu, L. Shi, M. S. Schmidt, A. Boisen, O. Hansen, J. Zi, S. Xiao, and N. A. Mortensen, *Nano Lett.*, **13**, pp 4690-4696 (2013).

[22] H. Da and C. W. Qiu, *Appl. Phys. Lett.* **100**, 241106 (2012).

[23] A. Vakil and N. Engheta, *Science* **332**, 1291-1294 (2011).

[24] X. Zou, J. Shang, J. Leaw, Z. Luo, L. Luo, C. Laovorakiat, L. Cheng, S. A. Cheong, H. Su, J. X. Zhu, Y. Liu, K. P. Loh, A. H. C. Neto, T. Yu, and E. E. M. Chia, *Phys. Rev. Lett.* **110**, 067401 (2013).

[25] H. Yan, Z. Li, X. Li, W. Zhu, P. Avouris, and F. Xia, *Nano Lett.* **12**, 3766-3771 (2012).

[26] S. Tani, F. Blanchard, and K. Tanaka, *Phys. Rev. Lett.* **109**, 166603 (2012).

[27] P. A. George, J. Strait, J. Dawlaty, S. Shivaraman, M. Chandrashekhar, F. Rana, and M. G. Spencer, *Nano Lett.* **8**, 4248-4251 (2008).

[28] J. M. Dawlaty, S. Shivaraman, M. Chandrashekhar, F. Rana, and M. G. Spencer, *Appl. Phys. Lett.* **92**, 042116 (2008).

[29] I. T. Lin, J. M. Liu, K. Y. Shi, P. S. Tseng, K. H. Wu, C. W. Luo, and L. J. Li, *Phys. Rev. B* **86**, 235446 (2012).

[30] I. Maeng, S. Lim, S. J. Chae, Y. H. Lee, H. Choi, and J. H. Son, *Nano Lett.* **12**, 551-555 (2012).

[31] L. Ju, B. Geng, J. Horng, C. Girit, M. Martin, Z. Hao, H. A. Bechtel, X. Liang, A. Zettl, Y. R. Shen, and F. Wang, *Nature Nanotechnology* **6**, 630-634 (2011).

[32] L. Ren, Q. Zhang, J. Yao, Z. Sun, R. Kaneko, Z. Yan, S. Nanot, Z. Jin, I. Kawayama, M. Tonouchi, J. M. Tour, and J. Kono, *Nano Lett.* **12**, 3711-3715 (2012).

[33] S. H. Lee, M. Choi, T. T. Kim, S. Lee, M. Liu, X. Yin,

H. K. Choi, S. S. Lee, C. G. Choi, S. Y. Choi, X. Zhang, and B. Min, *Nature Materials* **11**, 936-941 (2012).

[34] B. S. Rodriguez, R. Yan, M. M. Kelly, T. Fang, K. Tahy, W. S. Hwang, D. Jena, L. Liu, and H. G. Xing, *Nature Communications* **3**, 780 (2012).

[35] B. S. Rodriguez, T. Fang, R. Yan, M. M. Kelly, D. Jena, L. Liu, and H. Xing, *Appl. Phys. Lett.* **99**, 113104 (2011).

[36] L. Vicarelli, M. S. Vitiello, D. Coquillat, A. Lombardo, A. C. Ferrari, W. Knap, M. Polini, V. Pellegrini, and A. Tredicucci, *Nature Materials* **11**, 865-871 (2012).

[37] P. Liu, W. Cai, L. Wang, X. Zhang, and J. Xu, *Appl. Phys. Lett.* **100**, 153111 (2012).

[38] N. I. Landy, S. Sajuyigbe, J. J. Mock, D. R. Smith, and W. J. Padilla, *Phys. Rev. Lett.* **100**, 207402 (2008).

[39] N. Liu, M. Mesch, T. Weiss, M. Hentschel, and H. Giessen, *Nano Lett.* **10**, 2342-2348 (2010).

[40] C. Hägglund and S. P. Apell, *Optics Express* **18**, A343-A356 (2010).

[41] J. T. Liu, N. H. Liu, J. Li, X. J. Li, and J. H. Huang, *Appl. Phys. Lett.* **101**, 052104 (2012).

[42] N. M. R. Peres and Y. V. Bludov, *EPL* **101**, 58002 (2013).

[43] N. Laman and D. Grischkowsky, *Appl. Phys. Lett.* **93**, 051105 (2008).

[44] Changes in THz absorption are negligible if the 86 nm silver films are replaced by Al, Au, or thicker silver films.

[45] D. Grischkowsky, S. Keiding, M. Exter, and C. Fattiger, *JOSA B*, **7**, 2006-2015 (1990).

[46] M. Born and E. Wolf, *Principles of Optics* (Pergamon, Oxford, UK, 1989), pp. 38-74.

[47] K. Chang, J. T. Liu, J. B. Xia, and N. Dai, *Appl. Phys. Lett.* **91**, 181906 (2007).

[48] F. Blanchard, D. Golde, F. H. Su, L. Razzari, G. Sharma, R. Morandotti, T. Ozaki, M. Reid, M. Kira, S. W. Koch, and F. A. Hegmann, *Phys. Rev. Lett.* **107**, 107401 (2011).

[49] Y. V. Bludov, N. M. R. Peres, and M. I. Vasilevskiy, arXiv:1307.4096, Unusual reflection of electromagnetic radiation from a stack of graphene layers at oblique incidence

[50] B. Sensale-Rodriguez, R. Yan, S. Rafique, M. Zhu, M. Kelly, V. Protasenko, D. Jena, L. Liu, and H. G. Xing, *Infrared, Millimeter, and Terahertz Waves (IRMMW-THz)*, 2012 37th International Conference.

[51] W. Bao, F. Miao, Z. Chen, H. Zhang, W. Jang, C. Dames, and C. N. Lau, *Nature Nanotechnology* **4**, 562 - 566 (2009).

[52] W. Bao, K. Myhro, Z. Zhao, Z. Chen, W. Jang, L. Jing, F. Miao, H. Zhang, C. Dames, and C. N. Lau, *Nano Lett.* **12**, 5470-5474 (2012).